



## Aluminum alloys with high elastic modulus

J. Christudasjustus<sup>a</sup>, T. Larimian<sup>b</sup>, J. Esquivel<sup>c</sup>, S. Gupta<sup>d</sup>, A.A. Darwish<sup>a</sup>, T. Borkar<sup>b</sup>, R. K. Gupta<sup>a,\*</sup>

<sup>a</sup> Department of Materials Science and Engineering, North Carolina State University, Raleigh, NC 27606, United States

<sup>b</sup> Department of Mechanical Engineering, Cleveland State University, Cleveland, OH 44115, United States

<sup>c</sup> Department of Chemical, Biomolecular and Corrosion Engineering, The University of Akron, Akron, OH 44325, United States

<sup>d</sup> University Institute of Engineering and Technology, CSJM University, Kanpur, India

### ARTICLE INFO

#### Keywords:

Nanocrystalline materials  
Mechanical alloying  
Elastic modulus  
Nanoindentation  
Spark plasma sintering

### ABSTRACT

Binary Al-5M alloys, containing 5 at.% alloying element (M: Cr, Si, Nb, Mo, and V), have been produced by high-energy ball milling and subsequent spark plasma sintering. X-ray diffraction analysis indicated the solid solubility of the alloying elements to be several orders of magnitude higher than that predicted by the phase diagram. The elastic modulus and hardness of Al-5M alloys, analyzed using nanoindentation, were significantly higher than the commercial Al alloys. High elastic modulus was attributed to the decrease in lattice parameters as a result of the extended solid solubility of the alloying elements.

### 1. Introduction

Aluminum alloys possess a wide range of industrial applications due to their excellent manufacturability, lightweight, strength, and corrosion resistance [1]. However, the elastic modulus ( $E$ ) of Al alloys is significantly lower than other structural materials, which limits their use in applications requiring high stiffness. Therefore, research on increasing the elastic modulus of Al alloys is of great merit. Attempts to increase the elastic modulus of Al can be categorized as: 1) bimetallic structures [2], 2) composites with dispersion of ceramics [3], and 3) alloying [4]. Bimetallic and composite structures are not attractive choices due to deterioration in corrosion performance. Improving elastic modulus by alloying is a potential strategy which has not been explored much because of the limited solid solubility of most of the elements in Al and the limited effectiveness of conventional alloying elements in increasing elastic modulus. Recent work has shown effectiveness of high-energy ball milling (HEBM) in increasing the solid solubility of the non-conventional alloying elements in Al, which resulted in high corrosion resistance and strength [5–8]. These alloying elements were effective in decreasing the lattice parameter, which is reported to have substantial influence on the elastic modulus [9]. We present a hypothesis and its experimental validation that Al alloys with high elastic modulus can be produced by alloying with non-conventional alloying elements provided a solid solution is formed.

### 2. Materials and methods

Al-5M alloys were produced by HEBM of elemental powders in stainless-steel milling media followed by spark plasma sintering (SPS). HEBM was performed at 280 rpm for 100 h with a pause of 30 min after every 1 h of milling. Details of HEBM are presented in [6,10]. HEBM powders were consolidated using SPS at 200 °C under 1 GPa pressure for 5 min.

Scanning electron microscopy (SEM) and scanning transmission electron microscopy (S/TEM) were performed to characterize the microstructure. The specimens for SEM analysis were polished to a 0.05- $\mu\text{m}$  surface finish. The S/TEM specimens were prepared using focused ion (FIB) lift-out technique. The microstructure was studied using bright field (BF), dark field (DF), and high angle annular dark field (HAADF) imaging modes. The grain size through S/TEM was estimated using the DF images taken at (1 1 1) grain orientation from selected area electron diffraction (SAED) pattern. The X-Ray diffraction (XRD) analysis was conducted to analyze the grain size, solid solubility, and lattice parameter [6,11]. Cu  $K_{\alpha}$  radiation and the scan rate of 1°/min and 0.02° step size were used for XRD.

The nanoindentation was performed using Bruker Hysitron TI 980 to obtain the hardness and elastic modulus using 1000  $\mu\text{N}$  load and 10 s dwell time.

\* Corresponding author.

E-mail address: [rk Gupta@ncsu.edu](mailto:rk Gupta@ncsu.edu) (R.K. Gupta).

<https://doi.org/10.1016/j.matlet.2022.132292>

Received 2 December 2021; Received in revised form 28 March 2022; Accepted 15 April 2022

Available online 16 April 2022

0167-577X/© 2022 Elsevier B.V. All rights reserved.

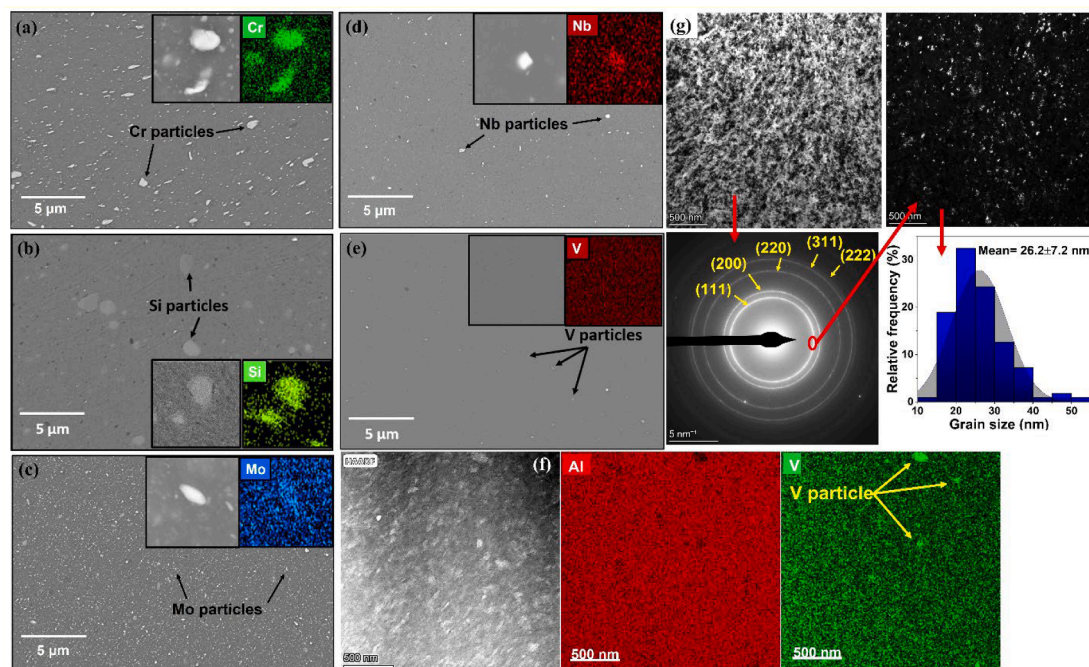


**Fig. 1.** Backscattered electron images and EDXS area maps of (a) Al-5Cr, (b) Al-5Si, (c) Al-5Mo, (d) Al-5Nb, (e) Al-5V alloys, (f) S/TEM-EDXS maps of Al-5V, and (g) TEM-BF and DF images with SAED pattern and grain size distribution.

### 3. Results and discussion

Backscattered electron (BSE) images for the Al-5M alloys revealed matrix and bright particles (Fig. 1a–e). High magnification BSE images along with the energy dispersive X-ray spectroscopy (EDXS) area maps of the alloying elements are presented as insets (Fig. 1a–e). The bright particles were confirmed to be rich in alloying elements, which were either unalloyed particles or secondary phases formed during HEBM. The sizes of the bright particles vary between 100 and 500 nm for V, Mo, and Nb, while 1–2  $\mu\text{m}$  for Si and Cr. EDXS point analysis revealed the matrix contained 5 at.% alloying elements (Supplementary section S1), which shows that added alloying element was distributed uniformly within the EDXS interaction volume. S/TEM analysis was performed on Al-5V alloy to demonstrate the microstructure at nanoscale. BF, DF, HAADF and selected area electron diffraction pattern (SAED) revealed nanocrystalline structure (Fig. 1g) and the grain size distribution is presented. EDXS area maps of V is presented to show the distribution (Fig. 1e). The V content of the matrix was close to 5 at.% that shows V was dispersed at nanoscale, which is a sign of high solid solubility.

X-ray diffraction revealed peaks corresponding to only Al along with significant peak shift towards high  $2\theta$  value, which indicated decrease in the lattice parameter. XRD peak position and peak broadening were used to calculate the lattice parameter and grain size (Supplementary section S2). The solid solubility of the alloying elements in Al-5M alloys was significantly higher than the values predicted by the phase diagram (Fig. 2a). For example, the solid solubility of V in Al-5V alloy was determined to be 2.75 at.%, which is  $\sim 10^6$  times higher than the equilibrium value. Grain size for all the alloys remained below 100 nm (Fig. 2a), which could be attributed to the short SPS time and lower temperature.

Hardness values are presented in Fig. 2b, which shows that Al-5M alloys presented herein exhibited superior hardness than any commercial Al alloy. The highest hardness was obtained for Al-5V (442 VHN), which is 1.5 times higher than high strength commercial alloy AA7075-T651 (supplementary section S2). The ability of alloying elements to increase the hardness was in the order of  $V > Mo > Nb > Si > Cr$ . The high strength of Al alloys was attributed to the grain refinements, precipitation hardening, and high solid solubility. The mechanism for

increased strength has been discussed in [10,12].

Elastic modulus ( $E$ ) of the Al-5M alloys, obtained using nano-indentation, was in the range of 79.84 to 95.89 GPa which is significantly higher than the commercial Al alloys (Fig. 2c). For example, elastic modulus of Al-5V alloy was 33% higher than that of AA7075-T651. Elastic modulus of Al-5M alloys along with that of commercial alloys is presented in Supplementary section S3. The influence of alloying elements in increasing elastic modulus was in the order of  $V > Mo > Nb > Si > Cr$ .  $E$  of the spark plasma sintered nanocrystalline (NC) Al was similar to that of and coarse-grained Al, indicating that the grain refinement does not have significant influence on the  $E$ , which is consistent with the literature [13,14].

The elastic modulus as a function of lattice parameter is presented in Fig. 3, which reveals that  $E$  increased with decrease in lattice parameter—the synergic effect of solid solubility and atomic radius mismatch. This experimental finding is consistent with the predictions from the first-principles calculations [15], which additionally showed the dependence on effective atomic radius (supplementary section S4). Introducing the substitutional solute into the pool of matrix atoms affects the lattice parameter of the alloy. Depending on the size of the solute atom and solubility the lattice parameter may expand or contract, which can be analyzed using XRD (supplementary section S3). Two factors – size of solute atom and the increase in solid solubility has decreased the lattice parameter of the Al crystal structure, which demonstrates the decrease in the interatomic spacing. This causes lattice mismatch and influences the bonding between the atoms. Therefore, observed elastic modulus could be expressed as a function of atomic radius of the solute and solid solubility of the alloying elements. Further mechanistic understanding requires first principles calculations and results presented herein can be used for theoretical predictions and developing strategies to develop Al alloys with high stiffness.

### 4. Conclusions

Al-5Cr, Al-5Si, Al-5Nb, Al-5Mo, and Al-5V alloys with high solid solubility of the alloying elements and grain size below 100 nm were produced by the HEBM and subsequent SPS. Lattice parameter for the Al-5M alloys was lower than that of Al. Elastic modulus and hardness of

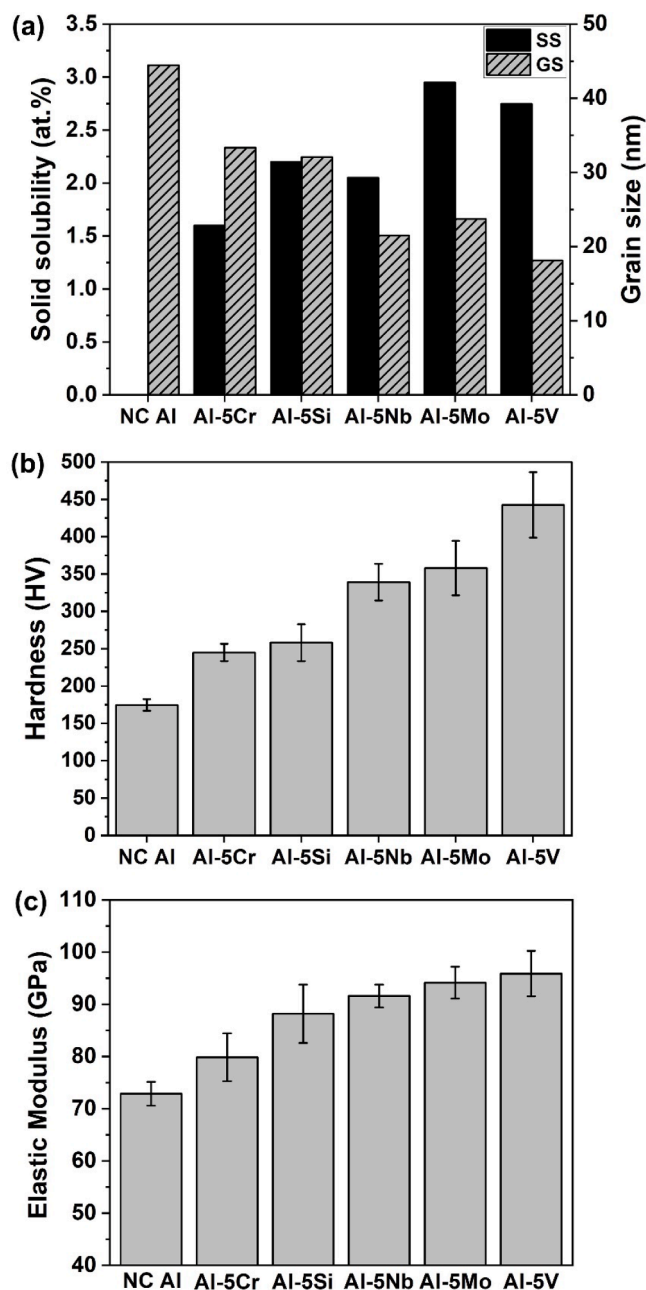


Fig. 2. (a) Solid solubility (SS) and grain size (GS) acquired from XRD data; (b) Hardness, and (c) Elastic modulus for Al-5M alloys.

Al-5M alloys were significantly higher than that of commercial Al alloys. The increase in elastic modulus in Al-5M alloys showed strong dependency on the lattice parameter, which is affected by the solid solubility and the effective atomic radius of the alloying elements. Effectiveness of alloying elements in increasing the elastic modulus was in the order of  $V > Mo > Nb > Si > Cr$ . This study shows that alloying of the appropriate elements resulting in supersaturated solid solution is an effective strategy to develop Al alloys with high elastic modulus.

#### CRedit authorship contribution statement

**J. Christudasjustus:** Writing – original draft, Writing – review & editing, Methodology, Data curation, Formal analysis, Investigation. **T. Larimian:** SPS. **J. Esquivel:** High-energy ball milling. **S. Gupta:** Data

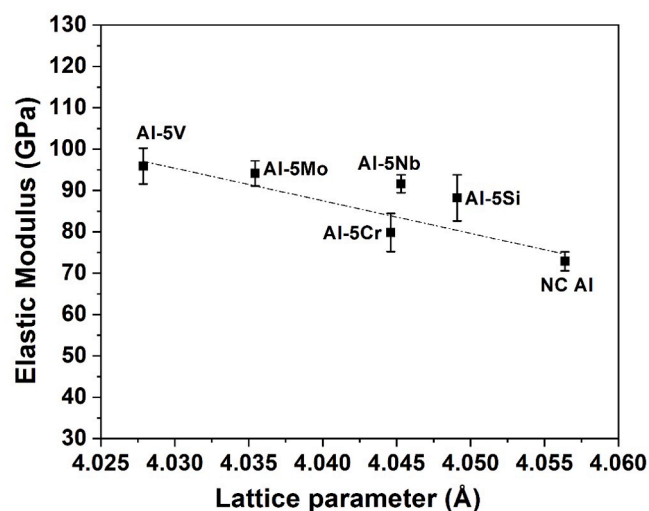


Fig. 3. Elastic modulus of Al-5M alloys as a function of lattice parameter.

analysis. **A.A. Darwish:** FIB and data analysis. **T. Borkar:** SPS. **R.K. Gupta:** Supervision, Writing – original draft, Writing – review & editing, Conceptualization, Methodology.

#### Declaration of Competing Interest

The authors declare that they have no known competing financial interests or personal relationships that could have appeared to influence the work reported in this paper.

#### Acknowledgement

The authors acknowledge the financial support from National Science Foundation (NSF-CMMI 1760204 and 2131440) under the direction of Dr. Alexis Lewis.

#### Appendix A. Supplementary data

Supplementary data to this article can be found online at <https://doi.org/10.1016/j.matlet.2022.132292>.

#### References

- [1] J.R. Davis (Ed.), *Corrosion of Aluminum and Aluminum Alloys*, ASM International, 1999.
- [2] S. Amirhanlou, S. Ji, *Crit. Rev. Solid State Mater. Sci.* 45 (2020) 1–21.
- [3] I.A. Ibrahim, F.A. Mohamed, E.J. Lavernia, *J. Mater. Sci.* 26 (1991) 1137–1156.
- [4] J.G. Kaufman, *Introduction to Aluminium Alloys and Tempers* (2000).
- [5] R.K. Gupta, B.S. Murty, N. Birbilis, *An Overview of High-Energy Ball Milled Nanocrystalline Aluminum Alloys*, Springer, 2017.
- [6] J. Esquivel, H.A. Murdoch, K.A. Darling, R.K. Gupta, *Mater. Res. Lett.* 6 (2018) 79–83.
- [7] J. Christudasjustus, C.S. Witharamage, G. Walunj, T. Borkar, R.K. Gupta, *J. Mater. Sci. Technol.* 122 (2022) 68–76.
- [8] L. Esteves, J. Christudasjustus, S.P. O'Brien, C.S. Witharamage, A.A. Darwish, G. Walunj, P. Stack, T. Borkar, R.E. Akans, R.K. Gupta, *Corros. Sci.* 186 (2021), 109465.
- [9] S. Münstermann, Y. Feng, W. Bleck, *Can. Metall. Q.* 53 (2014) 264–273.
- [10] C.S. Witharamage, J. Christudasjustus, R.K. Gupta, *J. Mater. Eng. Perform.* 30 (2021) 3144–3158.
- [11] A.L. Patterson, *Phys. Rev.* 56 (1939) 978–982.
- [12] R.K. Gupta, D. Fabijanic, T. Dorin, Y. Qiu, J.T. Wang, N. Birbilis, *Mater. Des.* 84 (2015) 270–276.
- [13] M. Abo-Elsoud, H. Esmail, M.S. Sobhy, *Radiat. Eff. Defects Solids* 162 (2007) 685–690.
- [14] T.D. Shen, C.C. Koch, T.Y. Tsui, G.M. Pharr, *J. Mater. Res.* 10 (1995) 2892–2896.
- [15] T. Uesugi, K. Higashi, *Comput. Mater. Sci.* 67 (2013) 1–10.